

Supplement of Biogeosciences, 15, 3439–3460, 2018
<https://doi.org/10.5194/bg-15-3439-2018-supplement>
© Author(s) 2018. This work is distributed under
the Creative Commons Attribution 4.0 License.



Supplement of

Evaluation of a new inference method for estimating ammonia volatilisation from multiple agronomic plots

Benjamin Loubet et al.

Correspondence to: Benjamin Loubet (benjamin.loubet@inra.fr)

The copyright of individual parts of the supplement might differ from the CC BY 4.0 License.

S1. Analogy between dispersion equation and flux-resistance approaches

It is interesting to note that **Eq. (1)** is essentially similar to resistance analogy approaches, where the flux F is evaluated as a concentration difference divided by a transfer resistance between two heights z_1 and z_2 , $F = -(C(z_2) - C(z_1))/R(z_1, z_2)$. Indeed, assuming, as is done in the resistance analogy that the source is infinitely expanded in x , then computing **Eq. (1)** for heights z_1 and z_2 and recombining leads simply to $R(z_1, z_2) = D(z_1) - D(z_2)$. Hence the transfer function D is equivalent to a transfer resistance. In particular, for infinitely expanded sources, the resistance between two heights equals the difference between the transfer function between these two heights and the ground.

S2 Condition number to identify suitable source-receptor geometry

A major issue when trying to infer sources from atmospheric concentrations is the fact that under some circumstances, the problem is ill-conditioned, which means that a small change in the concentration or the transfer matrix D_{ij} will induce large changes on the sources strength estimates. A measure of the conditioning of the problem is therefore an important indicator for determining whether the source-receptor geometry can lead to realistic solutions. The condition number is a measure of ill-conditioning and is defined as (Crenna et al., 2008):

$$CN = \|D_{ij}\| \times \|D_{ij}^{-1}\| \quad (\text{S1})$$

Where $\|\cdot\|$ denotes a norm of the matrix, one definition of which being the maximum of the sum of the rows. The higher CN , the larger the uncertainty on the solution of **Eqns. (3)** and **(6)** (Flesch et al., 2009). To evaluate the conditioning state of each set-up, we considered the simplified case where the background concentration is zero and the number of receptors equals the number of sources. In such a case, the matrix D_{ij} is squared and D_{ij}^{-1} is defined.

Considering the single source case eases the understanding of the meaning of condition number. Indeed, in that case $D_{ij} = D_j$ is a vector and CN is simply: $\max(\overline{D(x_i)})/\min(\overline{D(x_i)})$. In physical terms, this means that if some concentration samplers are well exposed to the source and others are not, CN is large. In such a case, **Eq. (4)** shows that a small error in $\overline{C(x_i)} - \overline{C_{bgd}}$ will lead to a large error in \overline{S} . Therefore we see here that using several concentration samplers may lead to increasing the error on \overline{S} if their locations are not chosen with care. This was also showed by Crenna et al. (2008) and Flesch et al. (2009), who showed that the condition number CN should be minimised in order to keep this error minimal; in this regards, Gao et al. (2008) suggest that CN should be smaller than 10. In practice, minimising CN would mean minimising the range of $\overline{D(x_i)}$. We can interpret this in terms of footprint: the source area should represent a reasonable footprint fraction of each concentration sensor. This holds for multiple sources also: in that case each source should represent a large fraction of each sensor footprint placed above it. The setup we propose in this study is, by construction, minimising CN as the sensors are placed in the middle of each plot, provided they are placed low enough to catch a significant part of the field footprint. If the plots are in a non-squared configuration, the CN is simply

calculated as in **Eq. S1**, where the second term in the right hand side is the pseudo inverse of the matrix D_{ij} . In practice, the calculation of CN was performed using the kappa function in R (version 3.2.3).

S3. Details of the FIDES model based on a solution of Philip (1959) of the advection diffusion equation

In the FIDES model, the transfer function $D(x_i, S_j, t)$ was estimated by first translating and rotating the x-y plan to locate the source S_j at the centre coordinates (0,0) and set the wind direction WD to 0 (align the x-axis with the wind vector). This was done by setting the following coordinate transformation $X_{ij} = (x_i - x_{s_j}) \sin(WD) - (y_i - y_{s_j}) \cos(WD)$, and $Y_{ij} = (x_i - x_{s_j}) \cos(WD) - (y_i - y_{s_j}) \sin(WD)$. Moreover, all heights are considered as heights above displacement height d ($Z = z - d$). In such conditions, the Philip (1959) solution reads:

$$U(Z_i) = aZ_i^p \quad (S2)$$

$$K_z(Z_i) = bZ_i^n \quad (S3)$$

$$D(x_i, S_j, t) = \frac{1}{\sigma_y(X_{ij})\sqrt{2\pi}} \exp\left(-\frac{(Y_{ij})^2}{2\sigma_y^2}\right) \times \frac{(Z_i Z_s)^{(1-n)/2}}{b\alpha X_{ij}} \times \exp\left(-\frac{a(Z_i^\alpha + Z_s^\alpha)}{b\alpha^2 X_{ij}}\right) \times I_{-\nu}\left(\frac{2a(Z_i Z_s)^{\alpha/2}}{b\alpha^2 X_{ij}}\right) \quad (S4)$$

$$\sigma_y = \frac{1}{\sqrt{2}} C_y X_{ij}^{\frac{2-m}{2}}$$

where $\alpha = 2 + p + n$, $\nu = (1 - n) / \alpha$, and $I_{-\nu}$ is the modified Bessel function of the first kind of order $-\nu$, and C_y and m were taken from Sutton (1932). The values of a , b , p and n were inferred by linear regression between $\ln(U)$, $\ln(K_z)$ and $\ln(Z)$, over the height range $2 \times z_0$ to 20 m, using $U(z)$ and $K_z(z)$ estimated from the Monin-Obukhov similarity theory as $K_z(Z) = ku_* Z [Sc \phi_H(Z/L)]^{-1}$. Here $\phi_H(Z/L)$ is the universal stability correction function as in Kaimal and Finnigan (1994), which is $\phi_H(Z/L) = (1 + 5.2 Z/L)$ for $Z/L \geq 0$ and $\phi_H(Z/L) = (1 - 16 Z/L)^{0.5}$ for $Z/L \leq 0$. Following Loubet et al. (2001), to ensure **Eq. (S4)** exists, the source height is taken as $Z_s = 1.01 z_0$. FIDES is essentially the same model as the one reported by Kormann and Meixner (2001). The only difference resides in the way a , b , p and n are determined: in Kormann and Meixner (2001) these constants are determined by equating U and K_z from Monin-Obukhov similarity theory to **Eqns. (S2 and S3)** at the reference height (H), while in FIDES a range of heights ($2 \times z_0$ to 20 m) is used to compute these values. However, Wilson (2015) shows that under neutral stratification, any choice of $H / z_0 \gg 10$ should return an adequate concentration profile near the surface at fetches $1 \ll x / z_0 \ll 10^5$, hence FIDES and Korman and Meixner models can be considered equivalent in the range of dimensions considered in this study.

S4. Insuring coherency between WindTrax and Philip (1959) models (tuning FIDES with WindTrax)

S4.1. Insuring comparable Schmidt numbers

The WindTrax software combines the backward Lagrangian stochastic (bLS) dispersion model described by (Flesch et al., 2004) with an interface where sources and sensors can be mapped. The transfer function $D(x_i, S_j, t)$ is calculated by releasing N trajectories upwind from each sensor location x_i for each time step and recording the

vertical velocity (w_0) of those that intersect the ground (N_{source} , or “touchdowns”). The transfer function is computed as:

$$D(x_i, S_j, t) = \frac{1}{N} \sum_{N_{\text{source}}} \left| \frac{2}{w_0} \right| \quad (\text{S5})$$

In practice $N = 50000$ trajectories were used to compute D_{ij} . In WindTrax the Schmidt number (Sc , see 2.2) tends to 0.64 in the neutral limit as discussed by Wilson (2015).

S4.2. Insuring comparable Schmidt numbers

Most bLS models, and especially WindTrax assume $Sc = 0.64$, while models based on the eddy diffusion analogy, and hence FIDES and the Korman and Meixner model, lead to a Sc which was calculated in Carozzi et al. (2013) to be:

$$Sc = \frac{u_*^2}{abp} Z^{1-p-n} \quad (\text{S6})$$

Hence constitutively, the Philip (1959) model does not lead to a constant Schmidt number in the surface layer, unless $1 - p - n \sim 0$, which was found to be the case under near neutral conditions (Carozzi et al., 2013). Note that the Korman and Meixner approach lead to $Sc = 1$ at the reference height in all conditions by construction. Furthermore, the stability correction functions are different in the Philip (1959) model and in WindTrax. Hence in order to compare the two approaches, the vertical diffusivity $K_z(Z)$ in FIDES was set as to reproduce the far field diffusivity of Flesch et al. (1995). Indeed, in bLS, the far-field diffusivity is $K_z = \sigma_w T_L$, where σ_w is the standard deviation of the vertical component of the air velocity, and T_L is the Lagrangian time scale. Replacing by their expression as in Flesch et al. (1995), leads to the following far-field diffusivity:

$$K_z(Z) = 0.5\sqrt{1.7}u_*Z / \left(1 + 5\frac{Z}{L}\right) \quad \text{for } L > 0 \quad (\text{S7})$$

$$K_z(Z) = 0.5\sqrt{2.2}u_*Z \times \left(1 - 6\frac{Z}{L}\right)^{0.25} \left(1 - 3.3\frac{Z}{L}\right)^{\left(\frac{0.67}{2}\right)} \quad \text{for } L \leq 0 \quad (\text{S8})$$

It is noticeable that in **Eqns. (S5 and S6)** there is a step change between stable and unstable conditions. Indeed, when $L \rightarrow +\infty$ $K_z(Z) \rightarrow ku_*Z \times 0.63^{-1}$, while when $L \rightarrow -\infty$ $K_z(Z) \rightarrow ku_*Z \times 0.55^{-1}$. This means that in WindTrax, the Sc number is set to 0.63 under stable conditions and 0.55 under unstable conditions and that in near-neutral conditions Sc steps from 0.63 to 0.55 when passing from $L > 0$ to $L \leq 0$.

In FIDES, to ensure compatibility with Flesch et al. (1995), Sc was set to 0.64 and parameters b / Sc and n were adjusted so that $K_z(Z)$ in **Eq. (S3)** fits that in **Eqns. (S7 and S8)** over a logarithmically spaced vector of 30 heights from $z_0 \times 1.01$ to 2 m. We should stress here that the expressions from Flesch et al. (1995) are slightly different from those in Windtrax (Flesch et al., 2004):

$$K_z(Z) = 0.5 \times 1.25 \times u_* Z / \left(1 + 5 \frac{Z}{L}\right) \quad \text{for } L > 0 \quad (\text{S9})$$

$$K_z(Z) = 0.5 \times 1.25 \times u_* Z \times \left(1 - 6 \frac{Z}{L}\right)^{0.25} \left(1 - 3 \frac{Z}{L}\right)^{1/3} \quad \text{for } L \leq 0 \quad (\text{S10})$$

From the **Eqns. (S9 and S10)** is noticeable that under near neutral situations ($L \rightarrow +\infty$ or $L \rightarrow -\infty$), the diffusivity $K_z(Z)$ is converges to $ku_*Z \times 0.64^{-1}$ (where $k = 0.41$ is the von Karman's constant and 0.64 represents the Schmidt number) and is continuous for all L . **Figure S1** based on **Eqns. (S9 and S10)** shows that our approach insures a coherency between the diffusivity of the bLS and Philip approach but small differences remain which are height dependent. We should also notice that lateral dispersion was treated separately in the two models, which will also lead to differences in the modelled concentration, especially for larger fields.

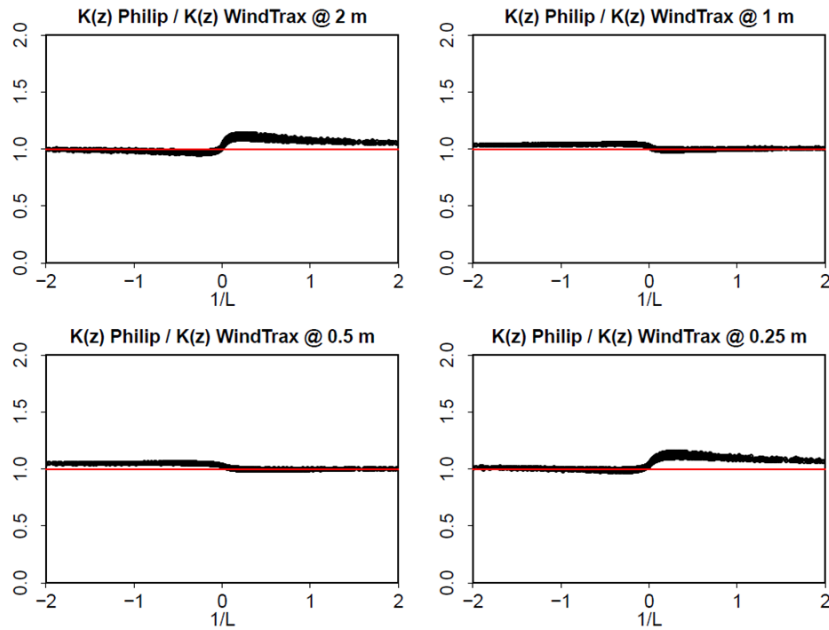


Figure S1. Ratio of the “tuned” FIDES (“Philip”) to WindTrax vertical diffusivity for scalars ($K_z(z)$) as a function of the inverse of Obukhov length ($1/L$) at 0.25, 0.5, 1 and 2 m heights. The tuned diffusivity corresponds to Eqns. (S9 and S10).

S4.3. Comparison of FIDES and WindTrax models for predicting concentrations above a single source

A first step in the study was to compare the two dispersion models. **Figure S2** shows that the “tuned” FIDES model leads to the same concentration pattern as WindTrax at 0.5 m above the source, although systematically underestimating the maximum concentration under unstable conditions. This behaviour is clearly visible in **Figure S3** where the concentrations modelled with the “tuned” FIDES at 2 m above the surface (right graph) are underrated by about 15% for unstable conditions compared to WindTrax, while matching for stable and neutral conditions. We further see that the concentration modelled with the original FIDES (Philip, 1959) are similar at 25 cm above the surface (left graphs) but differ substantially at 2 m above the surface (right graphs). This is expected as the longer the travel distance, the larger the expected difference in dilution if the two models' diffusivity differ. In the original FIDES, the diffusivity is lower than in WindTrax by a factor of roughly one and half ($Sc^{\text{Philip}} = 1$ and $Sc^{\text{WT}} = 0.64$). In a first order approach (over an infinitely homogeneous source), the

concentration difference between z_0 and 2 m would be proportional to the aerodynamic resistance (itself proportional to the inverse of the vertical diffusivity) times the height above ground (see e.g. Flechard et al., 2013), which explains the differences observed in **Figure S3**.

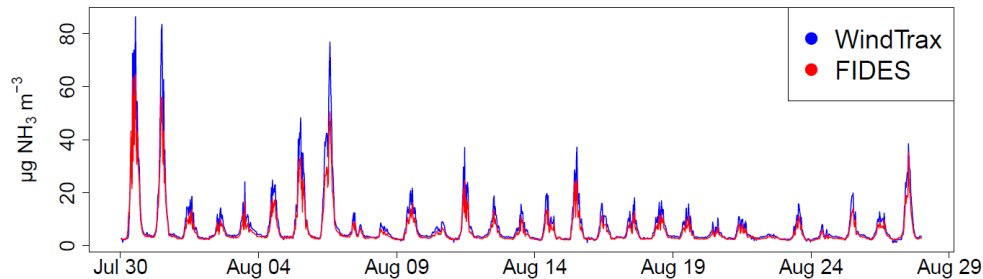


Figure S2. Example concentration modelled above a single ammonia source using two dispersion models WindTrax and FIDES with K_z as in Philip (1959), at 0.5 m above a simulated squared ammonia source of 25 by 25 m in the FR-Gri ICOS site during August 2008.

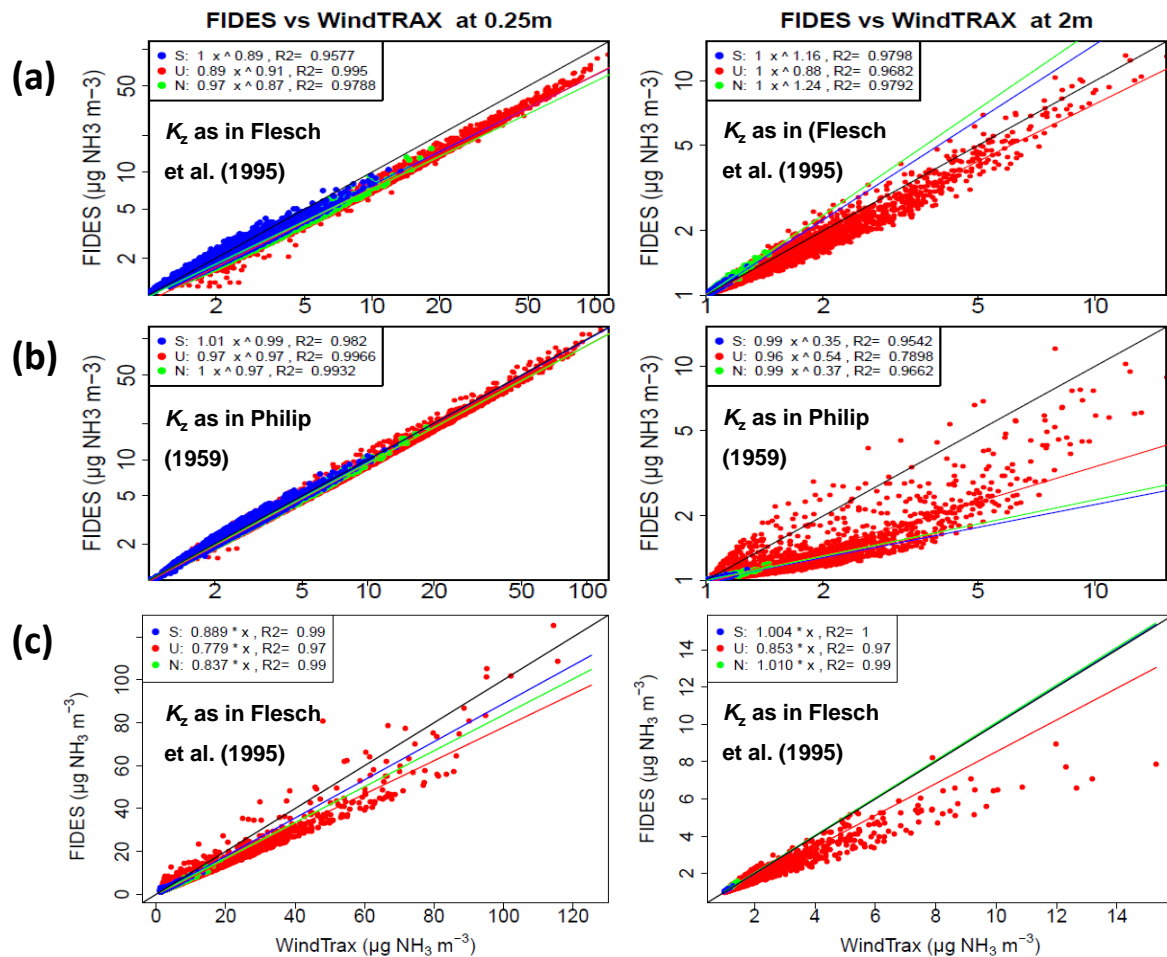


Figure S3. FIDES versus WindTrax concentration modelled above an ammonia source of 25×25 m at 0.25 and 2 m heights. In these graphs the FIDES vertical diffusivity K_z is either as in Philip (1959) (b) or fitted to Flesch et al. (1995) (a) and (c) as explained in S4.2. The comparison is made over the entire year of 2008 in the FR-Gri ICOS site. S, U and N stand for stable, unstable and neutral atmospheric conditions. The linear regression equation is given for each condition together with the R^2 of that regression. The black line is the 1:1 line. (a) and (b) show log-log axes and power law fits while (c) shows linear axes and linear fits.

Figure S3 also shows that the “tuned” FIDES modelled concentrations (top graphs) do not perfectly fit to the WindTrax ones (top graphs in **Figure S3**). At height of 25 cm, the “tuned” FIDES concentration does lead to a worse regression score than the original FIDES. Although **Figure S3** is focussing on a $25 \text{ m} \times 25 \text{ m}$ field, the results are similar for larger fields (data not shown). This is explained by the difference in Z -dependency of K_z in the WindTrax and FIDES model, which is highlighted in **Figure S1**: under stable conditions ($1/L > 0$), “tuned” FIDES $K_z(Z)$ is larger than WindTrax at 0.25 and 2 m, but smaller at 0.5 and 1 m, and the opposite under unstable conditions ($1/L < 0$). This means that constitutively the two models may never fit perfectly, showing a bias that will depend on height. Nevertheless, the correlation between the two models is very high as shown by large $R^2 \geq \sim 0.96$.

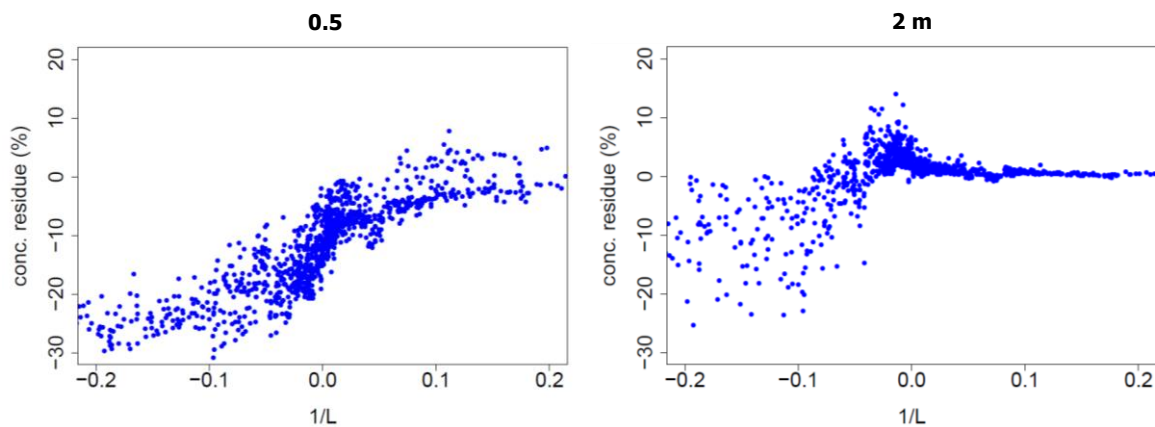


Figure S4. Relative difference between FIDES and WindTrax concentrations as a function of the stability parameter ($1/L$). Data refer to the same conditions reported in **Figure S3**.

Figure S4 reports the relative difference between the NH_3 concentration calculated by the two models at 0.5 and 2 m height, as a function of the stability parameter ($1/L$). As previously stated, under unstable conditions FIDES clearly underestimates the concentrations up to 30% at 0.5 m and lower heights, while this gap is reduced and more scattered at 2 m height. Moving towards neutral conditions the two models tends to agree notwithstanding an overestimation to 10% by WindTrax at 2 m height concurrently with an underestimation of the same magnitude by FIDES at 0.5 m. Under stable conditions there is a clear agreement at 2 m height, while this correspondence remains unbalanced to lower heights.

Supplementary figures

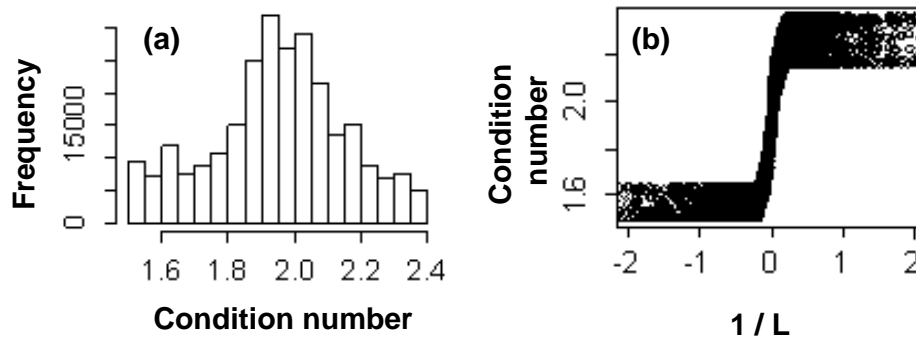


Figure S5. (a) Distribution of condition numbers for the 0.25 m height sensor and the 25 m width plots, for integration periods of 6h and 24h, and (b) condition number as a function of $1/L$, where L is the Obukhov length.

References quoted in the supplementary material

- Carozzi, M., Loubet, B., Acutis, M., Rana, G. and Ferrara, R.M., 2013. Inverse dispersion modelling highlights the efficiency of slurry injection to reduce ammonia losses by agriculture in the Po Valley (Italy). *Agric. For. Meteorol.*, 171: 306-318.
- Crenna, B.R., Flesch, T.K. and Wilson, J.D., 2008. Influence of source-sensor geometry on multi-source emission rate estimates. *Atmos. Environ.*, 42(32): 7373-7383.
- Flechard, C.R. et al., 2013. Advances in understanding, models and parameterizations of biosphere-atmosphere ammonia exchange. *Biogeosciences*, 10(7): 5183-5225.
- Flesch, T.K., Harper, L.A., Desjardins, R.L., Gao, Z.L. and Crenna, B.P., 2009. Multi-Source Emission Determination Using an Inverse-Dispersion Technique. *Boundary-Layer Meteorology*, 132(1): 11-30.
- Flesch, T.K., Wilson, J.D., Harper, L.A., Crenna, B.P. and Sharpe, R.R., 2004. Deducing ground-to-air emissions from observed trace gas concentrations: A field trial. *J. Appl. Meteorol.*, 43(3): 487-502.
- Flesch, T.K., Wilson, J.D. and Yee, E., 1995. Backward-Time Lagrangian Stochastic Dispersion Models and Their Application to Estimate Gaseous Emissions. *J. Appl. Meteorol.*, 34(6): 1320-1332.
- Gao, Z.L., Desjardins, R.L., van Haarlem, R.P. and Flesch, T.K., 2008. Estimating Gas Emissions from Multiple Sources Using a Backward Lagrangian Stochastic Model. *Journal of the Air & Waste Management Association*, 58(11): 1415-1421.
- Kaimal, J.C. and Finnigan, J.J., 1994. *Atmospheric Boundary Layer Flows, Their structure and measurement*. Oxford University Press., New York, 289 pp.
- Kormann, R. and Meixner, F.X., 2001. An analytical footprint model for non-neutral stratification. *Boundary Layer Meteorol.*, 99(2): 207-224.
- Loubet, B., Milford, C., Sutton, M.A. and Cellier, P., 2001. Investigation of the interaction between sources and sinks of atmospheric ammonia in an upland landscape using a simplified dispersion-exchange model. *J. Geophys. Res.-Atmos.*, 106(D20): 24183-24195.
- Philip, J.R., 1959. The Theory of Local Advection .1. *J Meteorol*, 16(5): 535-547.
- Sutton, O.G., 1932. A Theory of Eddy Diffusion in the Atmosphere. *Proceedings of the Royal Society of London. Series A*, 135(826): 143-165.
- Wilson, J.D., 2015. Computing the Flux Footprint. *Boundary Layer Meteorol.*, 156(1): 1-14.